"Bottom-up" Approach for Implementing Nano/microstructure Using Biological and Chemical Interactions

Sang Woo Lee[1], Woo-Jin Chang[2], Rashid Bashir[3], and Yoon-Mo Koo[2,4]*

[1] Department of Biomedical Engineering, College of Health Science, Yonsei University, Gangwon 220-710, Korea
[2] ERC for Advanced Bioseparation Technology, Inha University, Incheon 402-751, Korea
[3] School of Electrical and Computer Engineering, Weldon School of Biomedical Engineering, Birck Nanotechnology Center, Purdue University, West Lafayette, IN 47907, USA
[4] Department of Biological Engineering, Inha University, Incheon 402-751, Korea

Abstract The "Bottom-up" approach for implementing nano/microstructure using biological self-assembled systems has been investigated with tremendous interest by many researchers in the field of medical diagnostics, material synthesis, and nano/microelectronics. As a result, the techniques for achieving these systems have been extensively explored in recent years. The developed or developing techniques are based on many interdisciplinary areas such as biology, chemistry, physics, electrical engineering, mechanical engineering, and so on. In this paper, we review the fundamentals behind the self-assembly concepts and describe the state of art in the biological and chemical self-assembled systems for the implementation of nano/microstructures. These structures described in the paper can be applied to the implementation of hybrid biosensors, biochip, novel bio-mimetic materials, and nano/microelectronic devices. © KSBB

Keywords: bottom-up implementation, nano/microstructures, self-assembly, biomolecules

INTRODUCTION

Since a junction transistor was invented in 1947, one of the most important issues has been to reduce the size of the transistor. As a consequence, the cost of transistors is inversely proportional to the number of the electronic devices available from a silicon wafer. Many engineers and scientists have focused their researches on the manipulation of structures at the micro-/nano-scale. However, as the size of the structures has been reduced, the complexity and cost of fabrication have increased exponentially. Fig. 1 shows the trend of miniaturization of CMOS technology in last 30 years [1]. In 2005, a 0.05 μm minimum feature was achieved for the design of DRAM in mass production [2]. The continuity of this miniaturization trend is becoming difficult due to the limitations of conventional lithography, complexity of integration, physical phenomena, and so on.

On the other hand, nature has already perfectly controlled and manipulated micro-/nano-scale components using molecular recognition of various biological materials such as deoxyribonucleic acid (DNA), ribonucleic acid (RNA), protein, and cell. Those biological materials are self-assembled by molecular interactions [3,4]. The knowledge studied from nature can be used to solve the miniaturization issues. Moreover, engineers and scientists have applied this knowledge to implement artificial nano/microstructures used for detection and diagnostics [5-8], synthesis of new materials [9-11] and fabrication of novel electronic systems [12-15]. In this paper, the fundamental knowledge used for achieving artificial nano/microstructures is provided and the state of art for the implementation of the structures is reviewed. In addition, the future prospective issues used in the implementation of nano/microstructure are also discussed.

***Corresponding author**
Tel: +82-32-860-7513 Fax: +82-32-872-4046
e-mail: ymkoo@inha.ac.kr

BACKGROUND

Strategy for Achieving Nano/microstructures in Biological Self-assembly

There are two main forces in the molecular recognition process. One is a covalent bond consisting of carbon-carbon

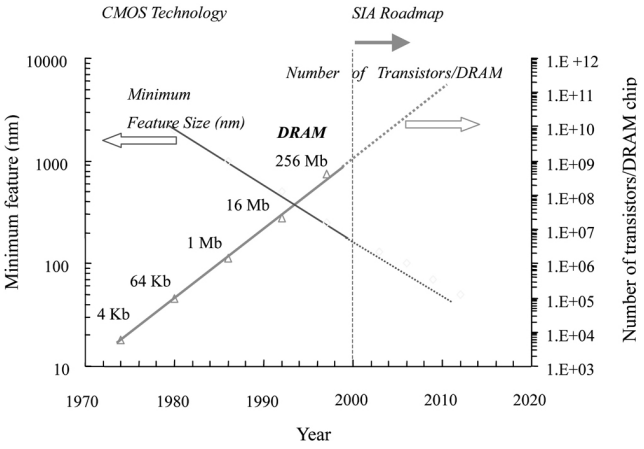

Fig. 1. The trend in miniaturization of integrated circuits (from [1]).

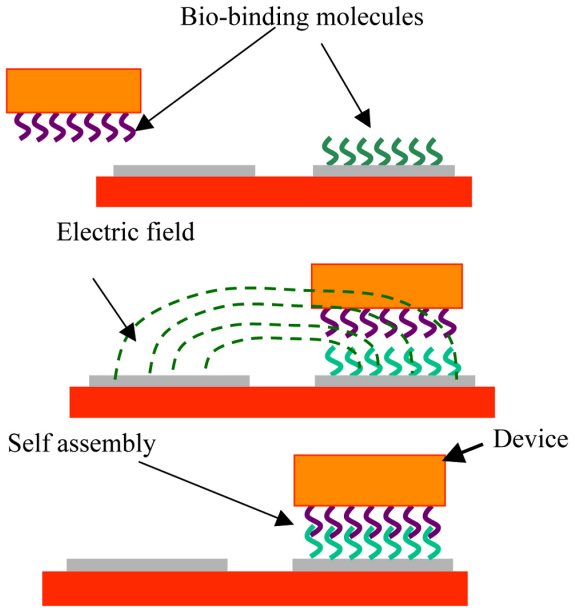

Fig. 2. The basic strategy to achieve nano/microstructures using electric field and bio-linkers.

molecules is well known and has an energy of 90 kcal/mol. The covalent bond plays a key role in binding the sub-units of the macromolecules. The other is a non-covalent bond which is much weaker than the covalent bond. Biological interactions typically depend upon the non-covalent bonds (*e.g.* hydrogen bond, ionic bond, van der Waals-London interaction and hydrophobic interaction).

Biomolecule-based self-assembly can be performed by three methods: DNA hybridization, ligand/receptor, or antigen/antibody interaction. In the case of DNA hybridization, a hydrogen bond provides the specificity behind the matching of complementary pairs of single-strand (ss) DNA to hybridize into a double-strand (ds). It has been estimated that each base pair binds with an energy of ~0.5 kcal/mol [16]. For an 18-mer oligonucleotide, the binding energy of a dsDNA can be estimated at 9 kcal/mol. However, the actual binding energy of a dsDNA is affected by the sequence of base-pair, salt concentration of surrounding media, temperature and other factors.

In the case of antibody/antigen or ligand/receptor interaction, binding takes place by a combination of ionic bonds, van der Waals-London interactions and hydrophobic interactions including multiple interactions. For example, avidin is a large protein that has binding sites for four biotin molecules. The affinity of the biotin/avidin complex is ~21 kcal/mol [17]. In comparison, the thiolate covalent bond between gold and thiol, which is used to attach thiol conjugated oligonucleotides on a gold surface, has an energy of 44 kcal/mol [18]. Although, taken individually, these energies are considerably less than those for many covalent single bonds (*e.g.* carbon-carbon interaction ~90 kcal/mol), they are sufficiently strong enough to provide stable attachment at ambient temperatures in composite.

The basic strategies used to implement artificial nano/microstrucutres are as follows: (i) attachment of biomolecules and its complementary molecules on a device and a specific binding site, respectively (ii) movement of the functionalized device close to the functionalized specific binding site due to physical forces such as gravity, mechanical agitation, electric force, magnetic force, and so on (iii) binding of two bio-linkers between the device and the specific binding site, resulting in artificial nano/microstructures. As shown in Fig. 2, a schematic diagram representing a strategy of which electric field as a physical force is used to bring a device to a specific binding site.

Scale Analysis of the Physical Forces for Achieving Nano/microstructures in Biological Self-assembly

In order to improve the efficiency of biological self-assembly, it is essential to bring devices functionalized by molecules into binding sites functionalized by its complementary molecules, resulting in the effective distance for biological interaction of the devices and the binding sites. Various physical forces such as gravity, mechanical agitation, magnetic force, and electric force can be used for it. However, in order to choose a proper force, it is really important to know a correlation between the physical forces and the biological self-assembled system, since the physical forces are changed as the scaling down of the system. The correlation between the physical forces and scale of nano/microdomain is discussed below. A single scale variable, S, is derived to represent the effect of force on the size of the biological self-assembled systems. The physical force that is responsible for the functionalized devices brought onto the binding site closely is described by the order of magnitude of S. For example, gravity acting on a particle with a diameter D is $F_{\text{gravity}} = \rho \frac{4}{3} \pi (\frac{D}{2})^3 g$, where ρ and g is the density of the object and an acceleration of the gravity, respectively. It is

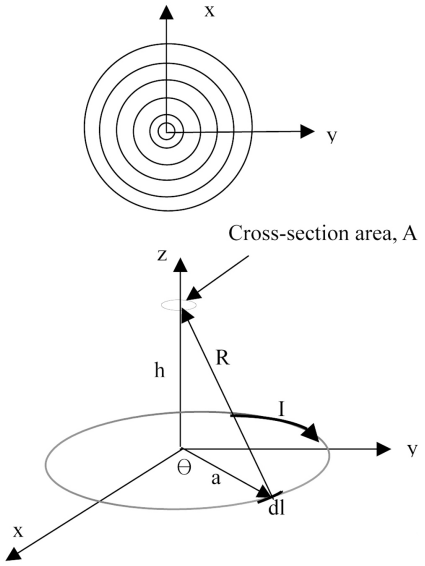

Fig. 3. The redrawn schematic diagram of a system with microcoils. (A) Top-view of the coils (B) the simplification to calculate scaling factor of a magnetic force (from [19]).

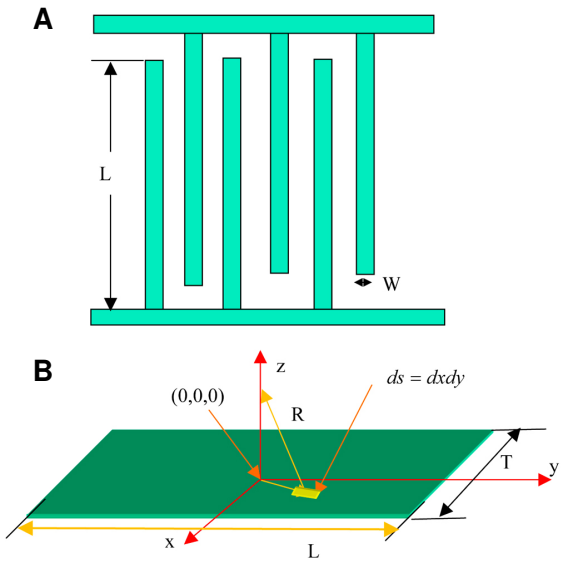

Fig. 4. The schematic diagram of a system consisting of interdigitated (IDT) electrodes. (A) Top-view of the IDT structure (B) the simplification to calculate scaling factor of an electrostatic force and a dielectrophoretic force.

clear that S^F (scaling factor of gravity) is S^3 since the gravity is decreased by a factor of a thousand when the diameter of the object is decreased ten times (ex. from 1.0 to 0.1 *D*). A scaling factor of a force is one of the most important aspects in deciding which physical force contributes to the implementation of nano/microstructures in biological self-assembly systems. In this section, three forces are discussed as examples.

Magnetic Force

The system with microcoils was considered [19] (Fig. 3). For simplification, only one microcoil was used to calculate the scaling factor of the magnetic force when a magnetic bead with a cross-section area, A, is located in the z-axis shown in Fig. 3B. The magnetic energy density, well known in electromagnetic theory, is $w_m = \frac{B^2}{2\mu_r}$ and the magnetic flux density (*B*) can be calculated by $\vec{B} = \oint d\vec{B}$. Since $d\vec{B}$ is $\frac{\mu_r I}{4\pi}\left(\frac{d\vec{l}\times\vec{R}}{R^3}\right)$ on the z-axis due to a current element $d\vec{l} = ad\theta\hat{\theta}$, $\vec{B} = \oint d\vec{B} = \frac{\mu_r I a^2 \hat{z}}{2(a^2+h^2)^{\frac{3}{2}}}$, where μ_r is a relative magnetic permeability, the distance between the current element and the cross-section area is: $\vec{R} = -a\hat{r} + h\hat{z}$, $\hat{r}$, $\hat{z}$, and $\hat{\theta}$ are unit vectors of each direction. In the first approximation, assuming the cross-section area is small enough compared to the area of the circular loop, the work to move the cross-section area into dz on the z-axis is expressed as: $dW_m = w_m A dz = \frac{\mu_r I^2 a^4}{8(a^6+h^6)} A dz$. Therefore, the magnetic force due to the circular loop is: $\vec{F} = -\frac{dW_m}{dz}\hat{z} = -\frac{\mu_r I^2 a^4}{8(a^6+h^6)} A\hat{z}$. Hence, since the current (*I*) is multiplied by current density (*J*) and the cross-section area ($I = JA$), the scaling factor of the current is: $S^I = S^2$. As a consequence, the scaling factor of magnetic force (S^F) in the system is: $S^F = \frac{(S^I)^2 S^4}{S^6} S^2 = S^4$.

Electrostatic Force

In the system consisting of an interdigitated (IDT) electrode structure, as shown in Fig. 4A, *W* and *L* are the width and length of the electrode, respectively. Since the IDT structure is repeated in several times, we can determine an electric field between two electrodes to figure out the electric field of all IDT structures by symmetry properties. Hence, we only consider the electric field of one electrode shown as Fig. 4B. The electric field in the z direction is: $\vec{E} = \frac{\sigma_A}{4\pi\varepsilon_r}\int_{-\frac{T}{2}}^{\frac{T}{2}}\int_{-\frac{L}{2}}^{\frac{L}{2}}\frac{\vec{R}}{R^3}dxdy$, where ε_r is a relative permitivity, the distance between the surface area ($dxdy$) in the x-y plane and a point (0, 0, z) on the z-axis is: $\vec{R} = -(x\hat{x} + y\hat{y}) + z\hat{z}$, $\hat{x}$, $\hat{y}$, and $\hat{z}$ are unit vectors of each direction, σ_A is a surface charge density of the electrode. Due to symmetric argument, the electric field is: $E = \frac{\sigma_A z}{4\pi\varepsilon_r}\int_{-\frac{T}{2}}^{\frac{T}{2}}\frac{L}{(x^2+z^2)[(\frac{L}{2})^2+x^2+z^2]^{\frac{1}{2}}}dx$. By definition of integration, the electric field can represent $E = \frac{\sigma_A z}{4\pi\varepsilon_r}\lim_{n\to\infty}\sum_{k=1}^{n}\frac{L}{(x_k^2+z^2)[(\frac{L}{2})^2+x_k^2+z^2]^{\frac{1}{2}}}\Delta x_k$. The calculation of

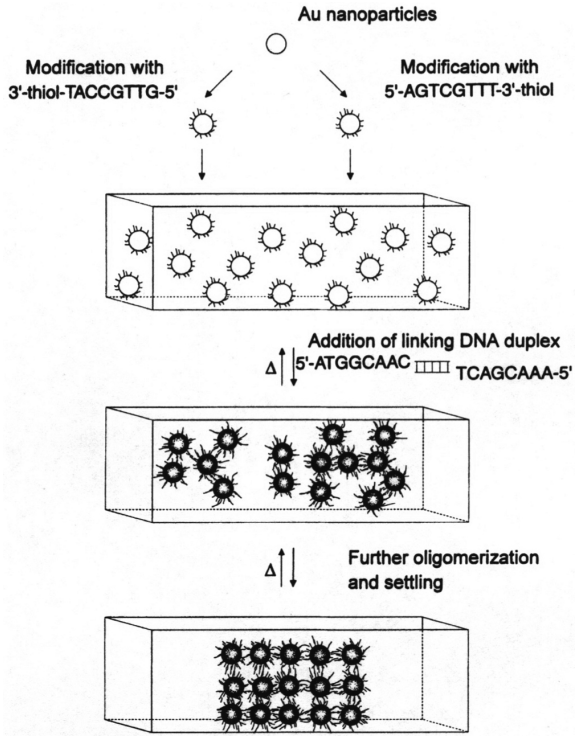

Fig. 5. Fabrication process for the aggregated assembly of DNA conjugated gold nanoparticles (from [10]). Reprinted, with permission, from Nature, Vol. 382, 15th August, 1996, p. 607. Macmillan Magazines Limited and with kind permission from C. Mirkin.

the scaling factor of E is enough to calculate the scaling factor of k^{th} component of the E, since E, is the summation of each component. Hence, The scaling factor of the electric field is: $S^E = S\dfrac{S}{(S^2+S^2)(S^2+S^2+S^2)^{1/2}}S = 1$. Assuming a charged particle is located at a point in the z direction above the center of the electrode, an electrostatic force described in the system shown in Fig. 4B is: $F = \dfrac{4}{3}\pi r^3 \rho E$, where r and ρ are the radius and charge density of the particle, respectively. Therefore, the scaling factor of electrostatic force (S^F) is $S^F = S^3 S^E = S^3$.

Dielectrophoretic Force

In case of a homogeneous spherical dielectric particle of α suspended in the solution subjected to an AC electric field of frequency ω, a dielectrophoretic force can be calculated by $F_{DEP} = 2\pi\varepsilon_m a^3 \,\mathrm{Re}[K(\omega)]\nabla|E_{RMS}|^2$ in the first approximation [20], where $\nabla|E_{RMS}|^2$ is the gradient of the square of the RMS electrical field, $K(\omega)$ called the Clausius-Mossotti factor is given by $K(\omega) = \dfrac{\tilde{\varepsilon}_p - \tilde{\varepsilon}_m}{\tilde{\varepsilon}_p + 2\tilde{\varepsilon}_m}$, $\tilde{\varepsilon}_p$ and $\tilde{\varepsilon}_m$ are the complex permitivities of the particle and the medium, respectively. Assuming the dielectrophoretic force acts on a particle located at a point in z direction above the center of the electrode as shown in Fig. 4B, the E_{RMS} can be used for the same equation driven in the above section, $E_{RMS} = \dfrac{\sigma_A z}{4\pi\varepsilon_r}\lim_{n\to\infty}\sum_{k=1}^{n}\dfrac{L}{(x_k^2+z^2)[(\frac{L}{2})^2+x_k^2+z^2]^{\frac{1}{2}}}\Delta x_k$. In addition, the dielectrophoretic force describes $F = 2\pi\varepsilon_0\varepsilon_m a^3 \,\mathrm{Re}[f_{CM}]\dfrac{\partial}{\partial Z}|E_{RMS}|^2$ since the field exists only in the z direction. Hence, $\dfrac{\partial}{\partial z}|E_{RMS}|^2$ becomes $\dfrac{\partial}{\partial z}\left|\dfrac{\sigma_A z}{4\pi\varepsilon_r}\lim_{n\to\infty}\sum_{k=1}^{n}\dfrac{L}{(x_k^2+z^2)[(\frac{L}{2})^2+x_k^2+z^2]^{\frac{1}{2}}}\Delta x_k\right|^2$. By the same argument described above, the scaling factor is $\dfrac{\partial}{\partial z}|S^E|^2 = \dfrac{1}{S}$. As a result, the scaling factor of dielectrophoretic force in the system is: $S^F = \dfrac{S^3}{S} = S^2$.

STATE OF ART

Four categories for the implementation of nano/microstrucure are reviewed in this section. The technique using DNA hybridization is described in the first section. Second category is protein mediated self-assembly for achieving nano/microstructure. Chemically mediated self assembled systems are presented in the third section. In the last section, electrically mediated self-assembly is introduced.

Nano/microstructure Using DNA Hybridization

Nanostructure Formed by DNA Self-assembly

The first demonstration of DNA mediated self-assembly was achieved in 1996 by Mirkin *et al.* and Alivisatos *et al.* [10,21]. The approach for self-assembly of DNA-functionalized gold nanoparticles is described in Fig. 5. Gold nanoparticles with a 13 nm diameter were separately functionalized in 3.75 μM (46 μL) of 3′-thiol-TACCGTTG-5′ and 3.75 μM (46 μL) of 5′-thiol-AGTCGTTT-3′-thiol solutions for 24 h. Following this step, two solutions containing gold nanoparticles, functionalized by non-complementary DNA, were combined and a DNA duplex solution such as 5′-ATGGCAACTATACGCGCTAG and 3′-ATATGCGCGATCTCAGCAAA was added into the solution to link the nano-gold colloids. After several hours, DNA-functionalized gold nanoparticles were aggregated. According to Mirkin *et al.* [24], thermal denaturation can be performed as temperature is increased. From this basic idea, several applications of gold nanostructures have been demonstrated. A binary nanoparticle network using DNA-directed synthesis was demonstrated by Mucic *et al.* [22]. The scheme to present the binary nanoparticle network was as follows: two different sized functionalized-DNA gold nanoparticles, whose diameters were 8 or 31 nm, were prepared in 3′-HS$(CH_2)_3$-OP(O)(O^-)-O-ATG-CTC-AAC-TCT and 3′-TAG-GAC-TTA-

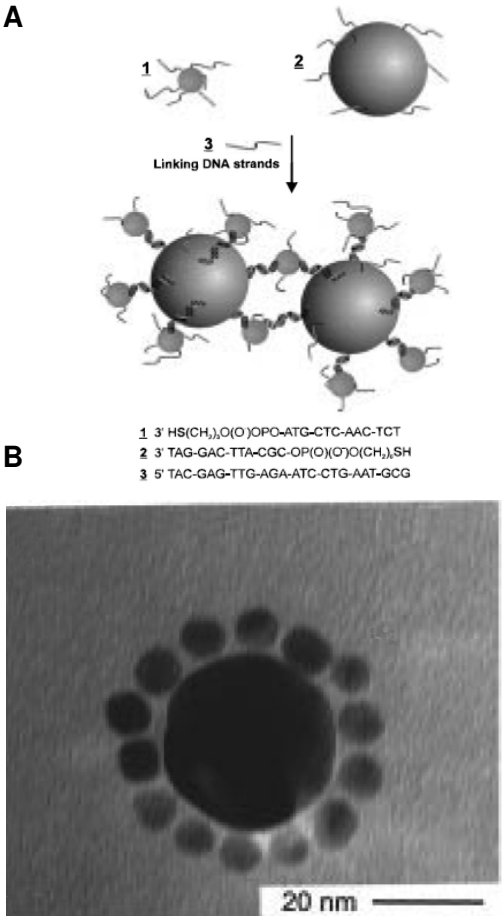

Fig. 6. Scheme of binary nanoparticles network and SEM image (A) schematic diagram for binary nanoparticles network. (B) Result after self-assembly using functionalized DNA (from [22]). Reprinted, with permission from J. Am. Chem. Soc. Vol. 120, p. 12674-12675, © 1998, American Chemical Society, and with kind permission from C. Mirkin.

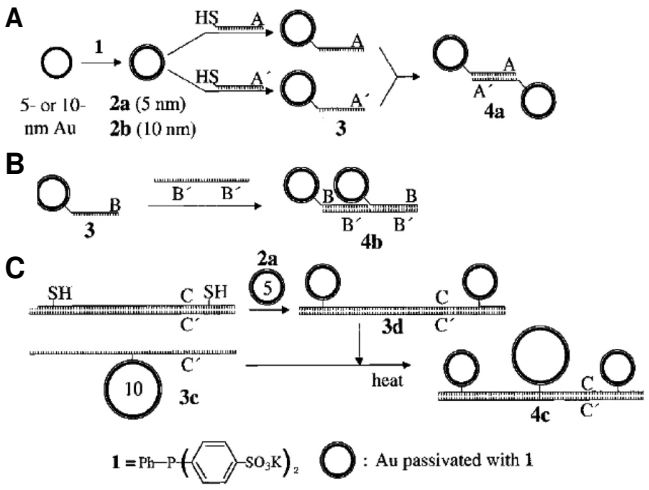

Fig. 7. The synthesis strategies for the description of gold nanoparticles (from [23]). Reprinted with perimission ftom Angew. Chem. Int. Ed. Vol 38, p. 1809, © 1999, Willey Interscience, and with kind permission from P. Alivisators.

CGC-OP(O)(O^-)$O(CH_2)_6SH$ solutions, respectively. A solution of 5′-TAC-GAG-TTG-AGA-ATC-CTG-AAT-GCG DNA strands were added to the mixture of two solutions in order to link the two different modified gold nanoparticles with the DNA strands. After several hours, a binary gold nanoparticle network was accomplished. Fig. 6 depicts the strategy of the binary nanoparticle network and the result after cross-linking. The use of gold nanocrystals has also been presented by Loweth *et al.* [23] using the complementary hybridization characteristics of DNA. The first approach in the demonstration of the use of gold nanocrystals was to directly combine modified-DNA gold nanoparticles with two complementary 5′-single strand DNA (Fig. 7A). The second method was to bind two gold nanoparticles coated with 5′-single strand DNA onto an unmodified template strand (Fig. 7B). In the last approach, the double and single stranded DNA, which had already been attached to two thiol groups and a gold nanoparticle, respectively, were utilized for the synthesis of gold nanoparticles of two different sizes (Fig. 7C). The authors showed heterodimers and homodimers with 5 and 10 nm gold nanoparticles using the three strategies described above.

One-dimensional gold nanoparticle arrays were demonstrated using rolling-circle polymerization and DNA-encoded self-assembly. Deng *et al*. [24] attached a gold nanoparticle (5 nm) into a DNA1 with a 5′ thiol group. Then, a lot of template DNA (T_{king}), complementary to the DNA1 attached on the gold nanoparticle, was combined with rolling-circle polymerization. The DNA (T_{king}) on the rolling-circle polymerization hybridized with the DNA1. As a result, long one-dimensional gold nanoparticle arrays were formed. Mirkin's group has also demonstrated the formation of supra-molecular nanoparticle structures where up to 4 layers of gold nanoparticles was produced. Using a single DNA strand, a particle coated by a complementary DNA was immobilized on an oxide surface. The linking DNA strand was attached on the particles to bind another layer of nanoparticles. When the procedures were repeated, a multi-layered network structures could be produced [25].

Since Seeman suggested to use DNA as scaffolds to serve as a framework for implementing nano-electronic devices, some applications of this idea have been reported by his group as follows [26-29]. The DNA tile shown in Fig. 8 is created using the following strategies: various structures such as DNA quadrilaterals, DNA knots, and Holliday junctions are designed with branched DNA and its complementary DNA (Fig. 8A) shows a stable branched DNA junction made by DNA molecules. If the hybridization region named the 'sticky ends' is provided in region B (Fig. 8B), a two-dimensional lattice can be also created using those DNA tiles. Seeman demonstrated that two-dimensional crystalline forms of DNA double cross-over molecules were programmed to self-assemble by the complementary binding of

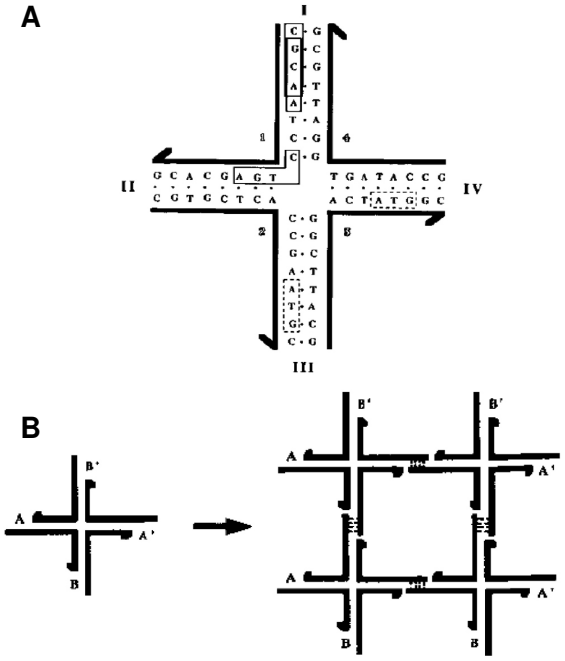

Fig. 8. Schematic diagram of DNA tile (A) A four-armed stable branched junction made from DNA molecules, (B) use of the branched junction to form periodic crystals (from [27]). Reprinted with permission, from Nanotechnology, © 1991, p. 149. IOP Publishing Limited, with kind permission from N.C. Seeman.

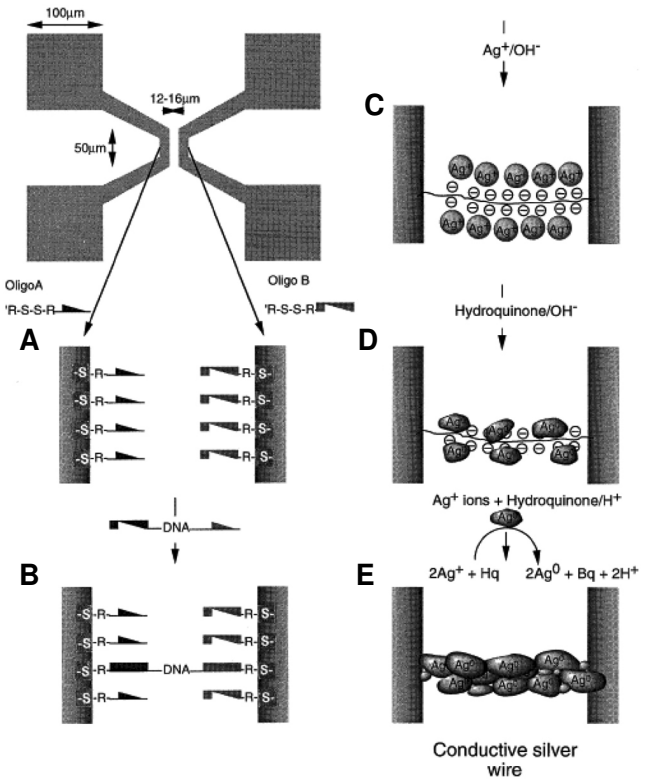

Fig. 9. The schematic diagram of conductive silver wire (from [33]). Reprinted, with permission from Nature, Vol. 391, p. 775, February, © 1998 Macmillan Magazine Limited and with kind permission from E. Braun.

the 'sticky ends' of the DNA molecules [29]. Rothemund *et al.* [30] showed that programmable DNA nanotubes were made from the DNA double-crossover molecules (DAE-E tiles), which had 7 to 20 nm diameters. Moreover, these tubes were assembled to each other so that they reached tens of microns in length at room temperature and split by heating, with an energy barrier around 180 k_bT [31]. DNA tiles shown were used for forming two dimensional and periodical gold nanoparticle arrays (Fig. 8) [32]. The method to demonstrate the arrays was the following: (i) 5 nm gold nanoparticles attached onto complementary DNAs of the DNA tiles (ii) complementary DNA with the gold nanoparticles hybridized with the DNA tiles (iii) DNA tiles with gold nanoparticles formed two dimensional periodic arrays as described in Fig. 8B. These lattices and tubes can also serve as scaffolding material for other biological materials.

Nano/microdevices Constructed by DNA Self-assembly

Braun *et al.* [33] demonstrated the conductive silver wire. Non-complementary hexane disulfide modified oligonucleotides were attached on two gold electrodes, which were separated by 12~16 μm, using thiol attachment. Then, a DNA bridge was formed using the complementary oligonucleotides. Subsequently silver ions were passed through the DNA bridge. Some of the silver ions were exchanged with sodium and remained on the DNA bridge. After hydroquinone treatment, silver ions on the bridge were aggregated and formed conductive silver wires. The experimental steps to make the conductive silver wire are described in Fig. 9. As a result, a silver wire of 100 nm diameter and 12 μm length was formed. DNA-templated gold wire has been developed by Keren *et al.* [34]. Firstly, single stranded DNA (ssDNA) and RecA monomer were polymerized, resulting in nucleoprotein filament (Fig. 10A). Consequently, the filament bound by aldehyde-derived double stranded DNA (dsDNA) substrate, as shown in Fig. 10B, is immersed into an incubated $AgNO_3$ solution. Ag was aggregated along with the substrate molecule except for the area protected by RecA (Fig. 10C). Finally, the aggregated Ag served as a catalyst for gold deposition and subsequently, conductive gold wire was formed on the unprotected region (Fig. 10D). A two-dimensional nanowire network was also demonstrated by DNA-templated self assembly [35,36]. The 4 × 4 DNA tile strand structure containing nine oligonucleotides which had four-arm junctions oriented in each direction (A, B, A′, B′) (Fig. 8B). Each junction had a T_4 loop which allowed the arms to point to four directions connecting adjacent junctions, was constructed, and each tile with the 'sticky end' of the tiles was connected, resulting in two-dimensional nanogrids and nanoribbons. To DNA metallization, the ribbons were seeded with silver using the glutaraldehyde method and sil-

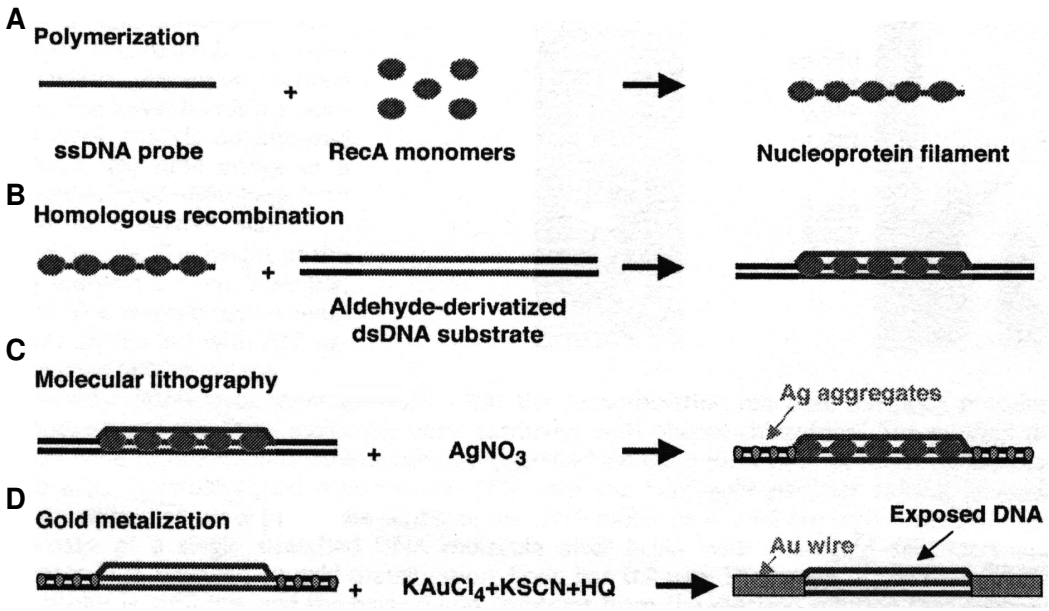

Fig. 10. Schematic diagram of the homologous recombination reaction and molecular lithography (from [34]). Reprinted with permission from Science Vol. 297, p. 72, © 2002, AAAS and with kind permission from E. Braun.

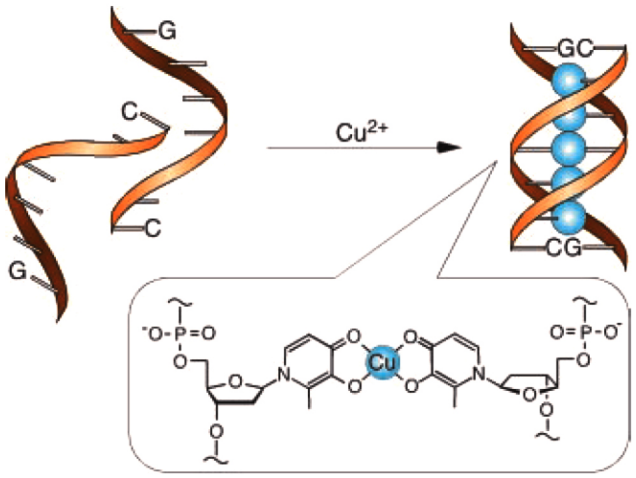

Fig. 11. Schematic diagram of Cu^{2+}-mediated duplex formation between two artificial DNA strands (from [38]). Reprinted with permission from Science Vol. 299, p. 1212, © 2003, AAAS with kind permission from M. Shionaya.

ver was deposited [37]. As a result, the nanoribbon which has a 43 nm [35] or 15 nm [36] diameter was formed.

Many researchers have been striving to develop materials that are used for molecular electronics, photo-detectors, fuel cells or field-effect-transistors by combining DNA with inorganic materials such as copper ions, acridine orange, Tin ions, or carbon nanotubes. Tanaka *et al.* [38] have synthesized an "artificial DNA" by copper ion-mediated base paring, which are a series of artificial oligonucleotides, d(5′-GH_nC-3′), with hydroxypyridone nucleobases (H) as flat bidentate ligands. Subsequently, copper ions were immersed into the artificial oligonucleotides and double helices of the oligonucleotides, nCu^+ d(5′-GH_nC-3′), were formed through copper ion base paring (H-Cu^+-H) (Fig. 11). A dye-DNA network [39] was incubated through mixing a DNA solution with an arcidine orange solution. The electrical conductivity of the network was enhanced while the sample was exposed to visible light. Application of the DNA composite membranes for a fuel cell was investigated by Won *et al.* [40]. Nano-porous polycarbonate membranes were modified with Tin (Sn) ions after immersing the membranes into a methanol/water solution (which contained $SnCl_2$ and CF_3COOH) for 45 min, followed by transferring them into a DNA solution. After 1 day, the membranes functionalized by DNA were irradiated with UV light in order to make cross-links of DNA film. As a result, the membranes with DNA film had high proton conductivity.

Carbon nanotube electronic devices implemented by DNA-inspired self-assembled techniques have obtained increasing attention. Hanzani *et al.* [41] have reported the assembly of single-walled carbon nanotubes (SWNTs) on gold electrodes using hybridization of DNA. The strategy of this approach is as follows: they incubated the self-assembled monolayers of DNA on gold electrode using 3′-thiolated oligonucleotides. Meanwhile, oxidized SWNTs with 3′-aminomodified oligonuleotides were prepared, immersed onto the electrode in order to achieve DNA hybridization and finally assembled on the gold electrodes. The multicomponent structure using carbon nanotubes and gold nanoparticles has been also described by Li *et al.* [42] using DNA hybridization techniques. Another approach using DNA-templated assembly in combination with RecA protein has been reported by Kinneret *et al.* [43]. In this approach,

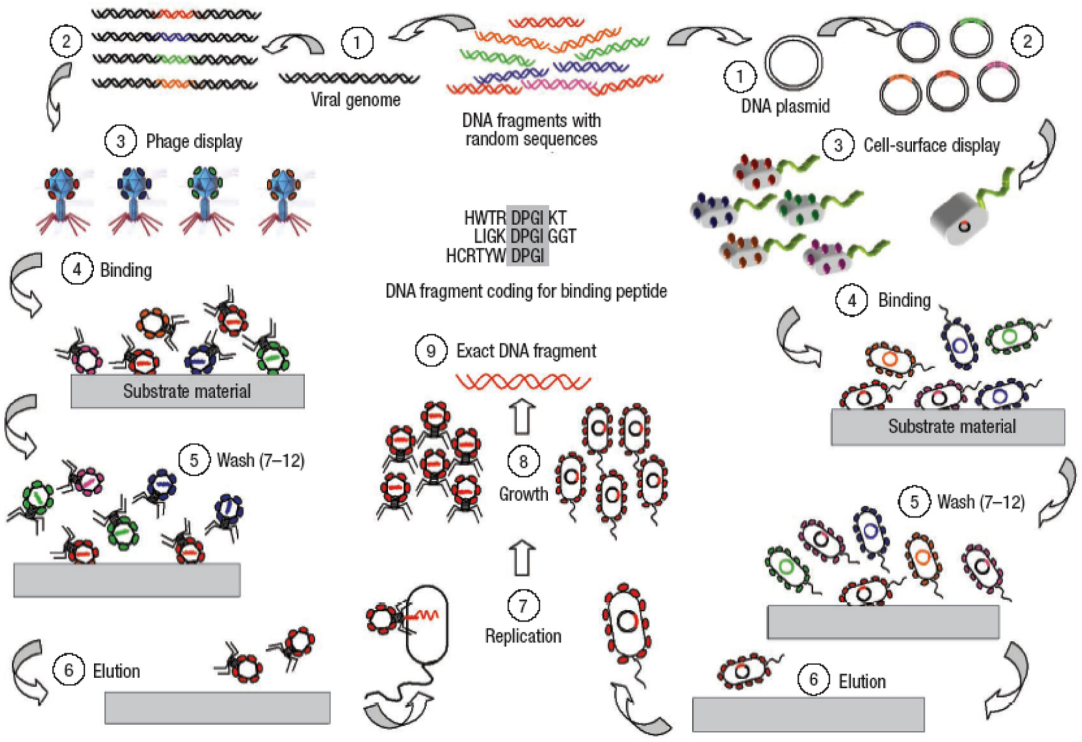

Fig. 12. Phase display and cell-surface display (from [44]). Reprinted, with permission from Nature Materials, Vol. 2, p. 680, © 2003 Macmillan Magazine Limited with kind permission from M. Sarikaya.

the precise localization of SWNTs working like a field effect transistor was implemented.

Nano/microstructure Using Protein Mediated Self-assembly

Genetically engineered polypeptides, which are defined as a sequence of amino acid for specially and selectively binding to an inorganic surface, can be used for the assembly of functional nanostructures as following: (i) inorganic-binding polypeptides are selected through display methods (ii) the selected polypeptides are modified by molecular biology to be used as linkers to bind nanoparticles, functional polymer or other nanostructures on molecular templates (iii) through self-assembly using modified polypeptides, ordered and multifunctional nanostructures can be implemented [44,45]. The most commonly used techniques to select the proper polypeptide for binding inorganic materials are phase display and cell surface display for the first step. That is, libraries are created through randomized oligonucleotides which are inserted into specific genes encoded on phase genomes or on bacterial plasmids (step 1 in Fig. 12). As a result, the randomized polypeptide sequence is incorporated within a protein residing on the surface of the organism (step 2 of Fig. 12). Eventually, each phase or cell produces and displays a different, but random peptide (step 3 in Fig. 12). Then, these phases or cells interacted on an inorganic substrate (step 4 in Fig. 12). After an intensive washing step, non-bound phases or cells are eliminated (step 5 in Fig. 12). Bound phases or cells are removed from the substrate (step 6 in Fig. 12). Then, the phases or cells are replicated and grown (step 7 in Fig. 12). Finally, DNA fragments for binding to the target substrate are extracted from the phases or cells. Using these display techniques, many researchers have developed binding sequences and implemented nanostructures. Using this technique, Belcher *et al.* [46] have reported bio-mediated synthetic material, selectively bonded on semiconductors. In their method, phase display libraries, which can supply 10^9 different peptides, were prepared for the binding of semiconductors. Meanwhile, different material substrates such as GaAs (100), GaAs (111) A, GaAs (111) B, InP (100), and Si (100) were prepared. Following this, the binding between peptides and substrates was accomplished and subsequently bound peptides were removed from the substrates. The binding procedure was then repeated under more constructed conditions until the phase achieving the most specific binding between peptides and substrates was found. Peptides selectively attached as material compositions or orientation differences were identified after repeating the method five times. Each peptide, in combination with the semiconductors, was selectively bonded on substrates. Brown *et al.* have demonstrated short Pt-and-Pd-binding sequences using cell surface display (CSD) [47]. The Ag binding sequences composed of 12 amino acids were developed by Naik *et al.* using phase display (PD) [48]. Moreover, metal-oxides binding sequences for ZnO [49], Zeolites [50], ZnS [51], and ionic

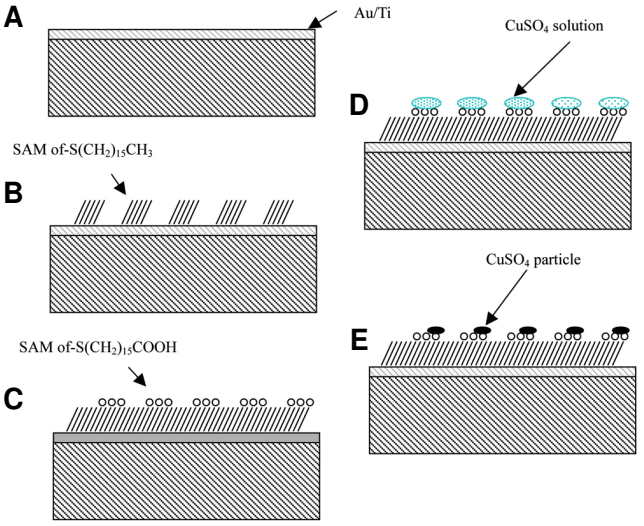

Fig. 13. The redrawn process flow for the demonstration of two ordered arrays of micro and nanoscale $CuSO_4$ particles (from [54]).

crystals binding sequences for $CaCO_2$ [52] and Cr_2O_3 [53] were reported using the phase display method.

Nano/microstructure Formed by Chemically Mediated Self-assembly

Nano/microstructure Implemented by Self-assembled Monolayers

Thiol groups are most often used for chemically mediated self-assemblies. Since thiol attaches well on a gold surface, a self-assembled monolayer (SAM) can be established on a gold surface after the reaction between the thiol group and the gold surface has been established. The functionalized-DNA gold nanoparticles mentioned above can also be accomplished by a thiol-gold reaction. As for the composition of molecules, self-assembled monolayers (SAMs) have different physical, chemical and electrical characteristics. Using these characteristics, researchers have developed three dimensional nano/microstructures. In the first category of chemically mediated self-assembly, SAMs are used as a medium for the integration of heterogeneous or homogeneous materials. Whitesides *et al.* [54], came up with a two-dimensional ordered array of nano/microparticles using a SAMs (Fig. 13). Titanium and gold was evaporated on a silicon substrate, sequentially, and a hydrophobic molecule, $HS(CH_2)_{15}CH_3$, was deposited on a gold surface using the micro-contact printing method. Subsequently, SAM-$S(CH_2)_{15}COOH$, which has hydrophilic properties, was made by washing the substrate in $HS(CH_2)_{15}COOH$ solution. The substrate was then dipped into the $CuSO_4$ solution for 1 min. The $CuSO_4$ solution remained on only SAM-$S(CH_2)_{15}COOH$ regions because SAM-$S(CH_2)_{15}COOH$ was hydrophilic. After the water was evaporated, $CuSO_4$ particles were assembled on the SAM-$S(CH_2)_{15}COOH$ region. As a result of the experiment, micro- and nano-$CuSO_4$ particles were placed on SAMs, which were carboxyl (–COOH) terminated (Fig. 13A~13D). Fig. 13E shows a schematic diagram after all procedures were completed, showing black dots, which are $CuSO_4$ particles, white dots which are a carboxyl (–COOH) terminated SAM and the remaining region representing a methyl ($–CH_3$) terminated SAM.

One of the most exciting discoveries in the field of nanotechnology is carbon nanotubes. These nanotubes, which are one of the most promising candidates to make nanoscale transistors and switches due to their unique electronic properties, are to implement an array using SAM. Rao *et al.* [55] applied polar chemical groups such as amino ($–NH_2$) and non-polar groups such as methyl ($–CH_3$) into a substrate such that two distinct regions were created on the substrate. After the substrate was immersed into a solution containing SWNTs, the nanotubes were attracted toward the polar regions and formed an aligned array. Another demonstration of SWNT arrays was also reported by Huang *et al.* [56]. However, there still remain a large gap between these nanotube array structures and the nanoscale circuit. This gap is one of the most important issues in nanotechnology today. As a consequence much work is needed in order to solve these issues.

Nano/microstructure Built by Capillary Force

The basic concept of chemically mediated self-assembly using capillary force was originally developed by Whitesides' group [57-60]. His group has demonstrated the concepts highlighting macro-scale plastic objects. The process of their method is firstly the synthesis of macro plastic pieces with the binding surface coated by alkanethiol precursor molecules. This molecules caused the binding surface to have the higher interfacial energy compared with the energy of water. High interfacial energy could make it energetically propitious for each patterned piece to join and self-align to minimize the exposed interfacial surface between the coated pieces and water. In the next step, the pieces were moved and agitated in water. Each coated surface was assembled by capillary force since the free energy between the coated surface of the pieces and the water was minimized after the assembly. Using the same concept, Jacobs *et al.* [61] fabricated a cylindrical display. GaAs/GaAlAs light emission devices (LEDs) with 280 × 280 × 200 μm assembled on the copper squares of a polyimide substrate so that two-dimensional array of LEDs was generated. His group also applied the same technique for the parallel assembly between LED segments and silicon carrier segments [62].

Capillary force was also used for forming micro-structures by Srinivasan *et al.* [63]. In this study, on the assembly of the micro-structures on the binding site, gold was evaporated on both the binding site of the substrate and micro-structures. Subsequently, SAMs were deposited only on the evaporated gold regions of the substrate and the micro-structures using alkanethiol precursor molecules. Following these procedures, the gold regions were hydrophobic with the remaining surface, covered by silicon dioxide, was hydrophilic. After introducing the micro-structures, the hydrophobic region of the

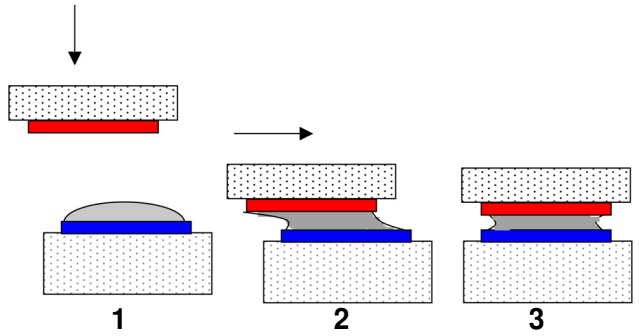

Fig. 14. The redrawn schematic diagram representing chemically mediated self-assembly using capillary force (from [63]).

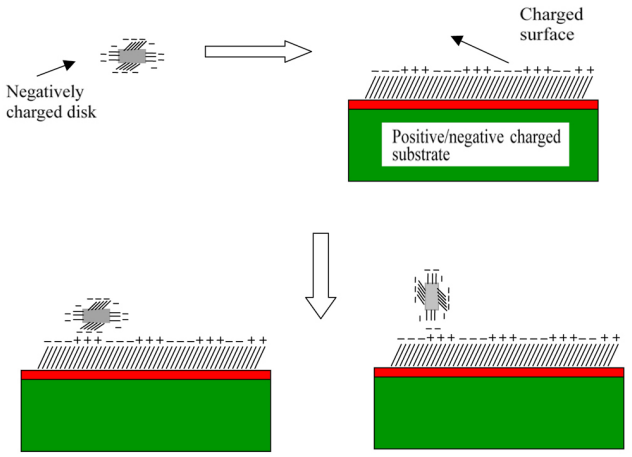

Fig. 15. The redrawn schematic diagram for electrostatic self-assembly (from [65]).

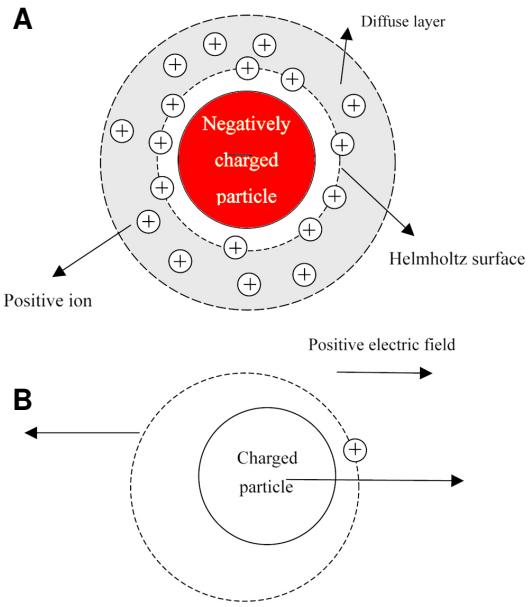

Fig. 16. The schematic diagram to explain electrophoresis.

micro-structures was assembled on the binding site of the substrate since the interfacial free energy was minimized when the hydrophobic region of the micro-structure was bonded on the binding site. The mechanism of this self-assembly is introduced in Fig. 14. As a result of self-assembly using capillary force, higher assembly yield and position precision were achieved. Micro-structures with a dimension of 400 × 400 × 50 μm and 150 × 150 × 15 μm were assembled on the binding sites of the substrate. The time for this self-assembly was less than 1 min with no defects (larger structures) or a 0.3° rotational misalignment and an alignment precision less than 0.2 μm (smaller structures). After self-assembly using the capillary force, heat or ultraviolet light was used for permanent bonding.

Nano/microstructure Created by Electrically Mediated Self-assembly

Electrokinetic effects as seen with electrostatic interactions, electrophoresis and dielectrophoresis are most widely used for improving efficiency of biological self-assembly as devices functionalized by biomolecules into a binding site coated by its complementary biomolecules are brought into use. These forces can be integrated and implemented within micro-TAS using fabrication techniques allowing the forces to be controlling its direction by providing polarity or frequency of a signal. In addition, the scaling factor of the electric field is usually $S^{-0.5}$ or S^{0} [64]. In this section, electrically mediated self-assembly using those electrokinetic effects is reviewed.

Whitesides *et al.* [65] has demonstrated an electrostatic self-assembled system attaching charged molecules into a device and a binding site. For electrostatic self-assembly, molecules which were terminated with cations or anions such as $COOH^{-}$ terminated SAM, PO_2H^{-} terminated SAM, NMe_2^{+} terminated SAM, or NH_2^{+} terminated SAM, were used for fabricating a charged substrate and charged micro-disks. Subsequently, the charged substrate was transferred into the solution containing negative or positive charged disks. The disks moved to the specific position on the substrate, which had oppositely charged SAMs, and were assembled by the electrostatic field (Fig. 15).

The charged particles suspended in a solution must be exactly balanced by an equal charge of the opposite polarity on the solution for electro-neutrality. Fig. 16A shows a schematic diagram to explain this phenomenon. When a negatively charged particle is in a solution where the region is closed to the partial surface containing the positive ions called the Helmholtz surface. The remaining positive charges are held in the region between the outer Helmholtz surface and the bulk of the solution, providing counter-ions for the rest of the charges on the particle. This region, called the diffused double layer, is created by the electrostatic interaction between the particles and ions in the solution. As shown in Fig. 16B, the charged particle and diffusion layer

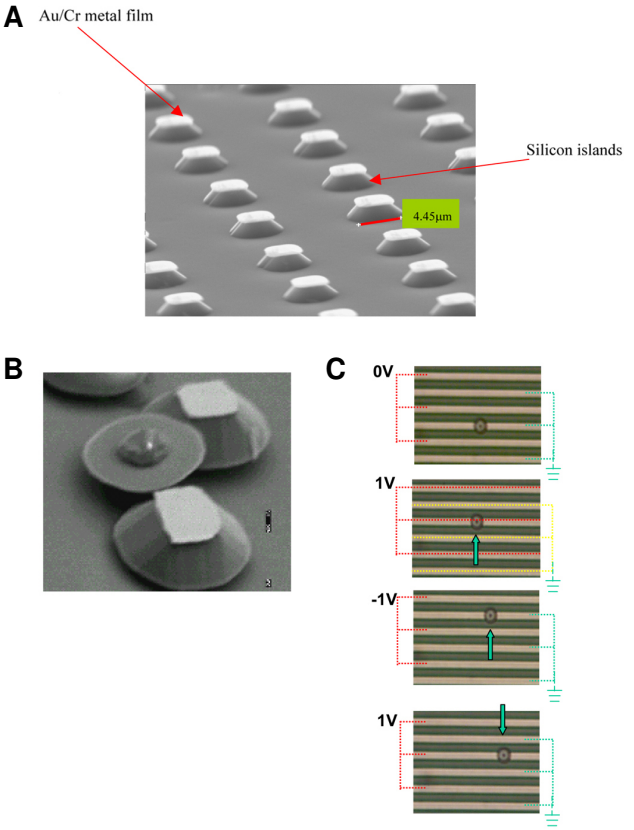

Fig. 17. The image of silicon islands. (A) The SEM image of the silicon islands on a silicon-on-insulator (SOI) substrate. (B) The SEM image after the release process. (C) The optical image representing electrophoretic movement.

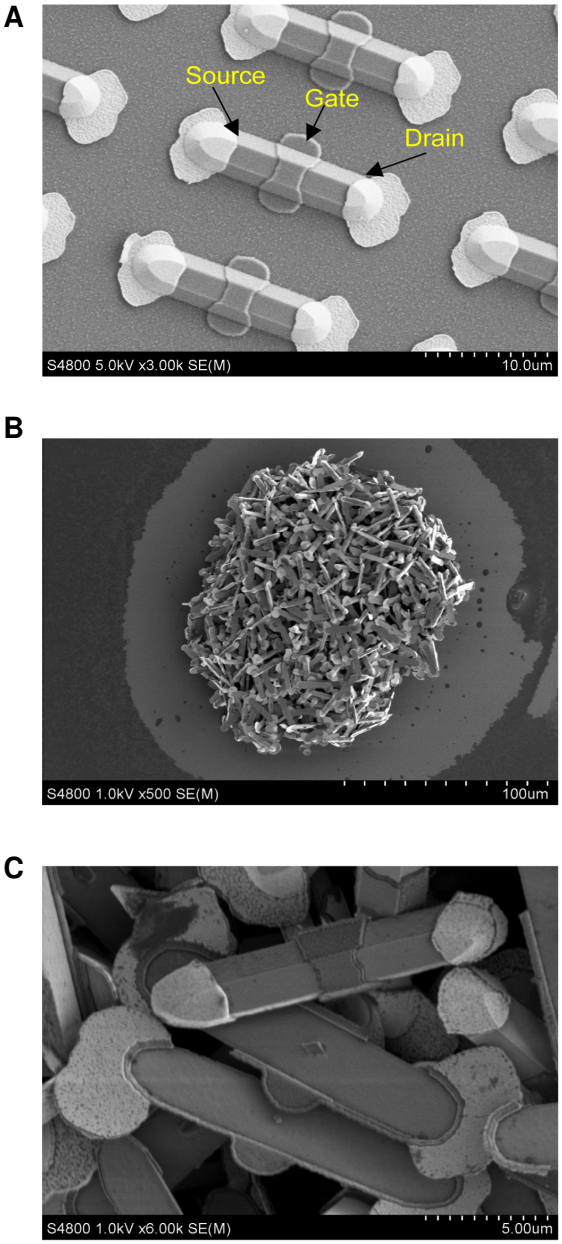

Fig. 18. The field emission scanning electron microscope (FESEM) images. (A) The completed silicon MOSFETs on BESOI Wafer. (B) FESEM pictures of an aggregate of devices after drying. (C) Close-up FESEM of the released device before assembly (from [15]).

are moved by applying voltage, which a well known principle of electrophoresis. Lee *et al.* [66] demonstrated the assembled system using electrophoresis. As shown in Fig. 17A, the trapezoidal shaped silicon islands with 4 × 4 μm thick gold/chromium layer at the top of the islands were fabricated. After the attachment of a 2-mercaptoethansulfonic acid sodium salt or the 4 nucleotide single stranded DNA to the gold surface, the islands were released from the substrate into DI water. Fig. 17B is confirmation of the release process. The islands can be moved into the specific binding site by electrophoretic forces. Fig. 17C shows the electrophoretic movement using the islands. Another example is O'Ridran *et al.* [67], who brought forward programmed self-assembly. They built 4 × 4 arrayed circular receptors with a 100 μm diameter and 250 μm pitch electrodes sites on a silicon substrate. A GaAs-based light emitting diode (LED) with 50 μm diameter was transported, positioned and localized on the selected binding site using the electric field. The various demonstrations using electrophoresis can be found in the literature. Heller's group used electrophoresis for capturing DNA strands at a specific site on biochips to implement DNA arrays [68-70]. An InGaAs LEDs with 20 μm diameter were assembled onto silicon circuitry using the electrophoretic effect [71].

Dielectrophoretic (DEP) force generated by to the interaction of a spatially non-uniform AC or DC field with a polarizable particle is explained in Li *et al.* [20]. In case of a homogeneous spherical dielectric particle with a radius (α), which is suspended in solution and subjected to an AC electric field with a frequency (ω), the time average DEP force represents $\overline{F}_{DEP} = 2\pi\varepsilon_m a^3 \mathrm{Re}[K(\omega)]\nabla|\overline{E}_{rms}|^2$, where $\nabla|\overline{E}_{rms}|^2$ is

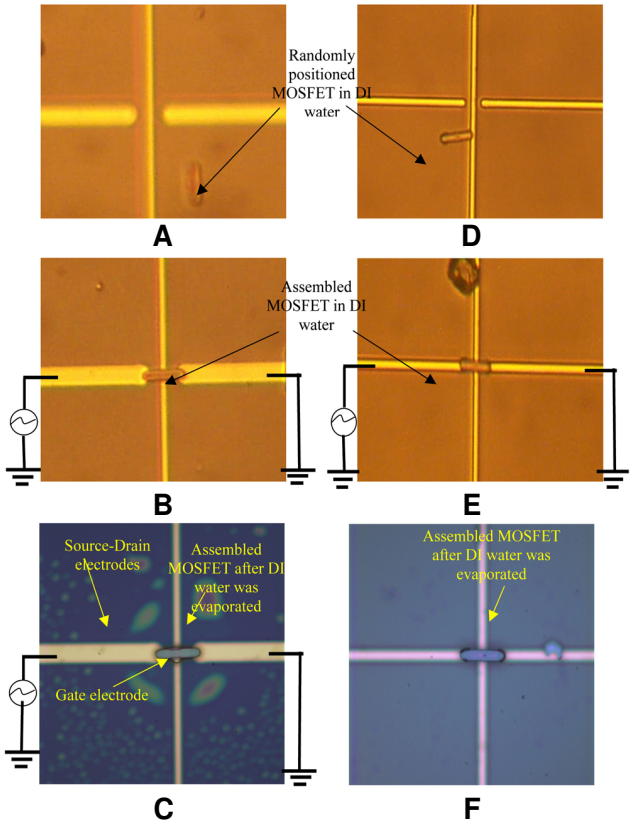

Fig. 19. Non-functionalized electrode. (A) Randomly distributed silicon MOSFET in DI water (0.05% Tween-20) before AC signal is on. (B) Assembled silicon MOSFET in DI water after AC signal is on. (C) Assembled silicon MOSFET after DI water is completely dried, where the AC signal was on during the drying process. Functionalized electrode. (D) Randomly distributed silicon MOSFET in DI water (0.05% Tween-20) prior to application of AC signal. (E) Assembled silicon MOSFET in DI water following application of AC signal. (F) Assembled silicon MOSFET showing a good alignment after complete evaporation of the DI water, where the AC signal was off during the drying process (from [15]).

the gradient of the square of the root mean square (RMS) electrical field. Re[$K(\omega)$] called the real value of the Clausius-Mossotti factor is obtained by $\mathrm{Re}[K(\omega)] = \mathrm{Re}[\frac{\tilde{\varepsilon}_p - \tilde{\varepsilon}_m}{\tilde{\varepsilon}_p + 2\tilde{\varepsilon}_m}]$. $\tilde{\varepsilon}_p$ and $\tilde{\varepsilon}_m$ are the complex permitivities of the particle and the medium, respectively. At Re[$K(\omega)$] > 0, the DEP force is positive. Otherwise, the DEP force is negative. When the DEP force is positive, the particle suspended in the solution moves toward the maximum electrical field gradient. In the negative DEP force, the suspended particle moves toward the minimum electric field gradient. This effect has been used to assemble and align metallic nanowires within patterns of interdigitated electrode arrays [72]. The self-assembly using silicon islands and resistors [73,74] has also been demonstrated using dielectrophoresis and chemically mediated self-assembly of three terminal of a single-crystal silicon metal-oxide-semiconductor field effect transistor [15]. The devices with 2 μm width, 15 μm length, and 1.3 μm thickness were fabricated on a SOI wafer and successfully released from an original substrate into DI water (Fig. 18). Following this, the devices suspended in DI water were assembled on an exact binding position using DEP force and the force combining dielectrophoretic force and molecular binding (Fig. 19). The electrical characteristics such as transfer (V_{ds} vs. I_{ds}) and output (V_{ds} vs. I_{ds}) of the assembled device was also measured and analyzed.

CONCLUSION

In this paper, we described the fundamental and the state of art of the bottom-up approach in accomplishing nano/microartificial structures. The four interactions, such as the hydrogen bond, ionic bond, van der Waals-London interaction, and hydrophobic interaction, play important roles on a biological self-assembly. For example, a hydrogen bond is favored for achieving DNA hybridization. Protein mediated self-assembled systems can be accomplished in combination with ionic bonds, van der Waals-London interactions, and hydrophobic interactions. The scaling analysis is also an important issue when micro-TAS is built using the nano/microstructures since the physical forces improving efficiency of the self-assembled system are dependent on the size of the system. The techniques described in the section 3 have been accomplished for the last ten years and are still under development. In the field of nano/biotechnology, the artificial nano/microstructures generated by biomolecules have a tremendous impact. Gold clusters and metal rods introduced in the section 3 can be used for passive electronic components. Carbon nanotubes [75,76], silicon nanowires [77-79] and the silicon metal-oxide-semiconductor field effect transistor (MOSFET) are potential candidates for the implementation of an active electronic circuit. Flexible display can be implemented by chemical mediated self-assembly, and the system using biomolecules can be used for implementing biochips for detection and diagnostics [80]. Moreover, the integrated system using the passive, active, display electronic component, and biochips can be possibly built by the bottom-up approach described here. However, there remains many issues that have to be resolved, such as, how parallel assembly of a large number of devices can be performed, how individual nanoelectronic component such as the carbon nanotubes and silicon nanowires can be put together, resulting in the integrated circuits, and how individual biosensors can be hybridized with a silicon CMOS chip. Furthermore, even though the issues described above are solved, there is still a large gap between prototype devices developing/developed in laboratories and devices in mass production. The development of technology for the implementation of the devices with high yield, high reliability, and low cost is critical issue in this area within near future.

Received January 16, 2007; accepted March 21, 2007

REFERENCES

1. Bashir, R. (2001) DNA-mediated artificial nano-bio-structures: state of the art and future directions. *Superlattice Microstructures* 32: 1-16.
2. Samsung Electronics (2005) www.samsung.com/Press Center/PressRelease. September 12. Seoul, Korea.
3. Park, J. W., H. S. Jung, H. Y. Lee, and T. Kawai (2005) Electrical recognition of label-free oligonucleotides upon streptavidin-modified electrode surfaces. *Biotechnol. Bioprocess Eng.* 10: 505-509.
4. Park, T. J., J. P. Park, S. J. Lee, H. J. Hong, and S. Y. Lee (2006) Polyhydroxyalkanoate chip for the specific immobilization of recombinant proteins and its applications in immunodiagnostics. *Biotechnol. Bioprocess Eng.* 11: 173-177.
5. Heller, M. J., A. H. Forster, and E. Tu (2000) Active microelectronic chip devices which utilize controlled electrophoretic fields for multiplex DNA hybridization and other genomic applications. *Electrophoresis* 21: 157-164.
6. Gilles, P. N., D. J. Wu, C. B. Foster, P. J. Dillon, and S. J. Chanock (1999) Single nucleotide polymorphic discrimination by an electronic dot blot assay on semiconductor microchips. *Nat. Biotechnol.* 17: 365-370.
7. Gupta, A., P. Nair, D. Akin, S. Broyles, M. Ladisch, A. Alam, and R. Bashir (2006) Anomalous resonance in a nanomechanical biosensor. *Proc. Natl. Acad. Sci. USA* 103: 13362-13367.
8. Johnson, L., A. Gupta, D. Akin, A. Ghafoor, and R. Bashir (2006) Detection of vaccinia virus mass using micromechanical cantilever sensors. *Sens. Actuators B Chem.* 115: 189-197.
9. Seeman, N. C. (1998) DNA Nanotechnology: novel DNA constructions. *Annu. Rev. Biophys. Biomol. Struct.* 27: 225-248.
10. Mirkin, C. A., R. L. Letsinger, R. C. Mucic, and J. J. Storhoff (1996) A DNA-based method for rationally assembling nanoparticles into macroscopic materials. *Nature* 382: 607-609.
11. Chan, W. C. W. and S. Nie (1998) Quantum dot bioconjugates for ultrasensitive nonisotopic detection. *Science* 281: 2016-2018.
12. Gu, J., S. Tanaka, Y. Otsuka, H. Tabata, and T. Kawai (2002) Self-assembled dye-DNA network and its photoinduced electrical conductivity. *Appl. Phys. Lett.* 80: 688-690.
13. Zheng, W., P. Buhlmann, and H. O. Jacobs (2004) Sequential shape-and-solder-directed self-assembly of functional microsystems. *Proc. Natl. Acad. Sci. USA* 101: 12814-12817.
14. Jacobs, H. O., A. R. Tao, A. Schwartz, D. H. Gracias, and G. M. Whitesides (2002) Fabrication of a cylindrical display by patterned assembly. *Science* 296: 323-325.
15. Lee, S. W. and R. Bashir (2005) Dielectrophoresis and chemically mediated directed self-assembly of micron scale 3-terminal MOSFETs. *Adv. Mater.* 17: 2671-2677.
16. Prohofsky, E. (1995) *Statistical Mechanics and Stability of Macro-Molecules: Application to Bond Disruption, Base Pair Separation, Melting, and Drug Dissociation of the DNA Double Helix.* Cambridge University Press, New York, NY, USA.
17. Richards, F. M. (1990) Reflections. *Methods Enzymol.* 184: 3-5.
18. Ulman, A. (1996) Formation and structures of self-assembled monolayers. *Chem. Rev.* 96: 1533-1554.
19. Chiou, C.-H., Z.-F. Tseng, and G.-B. Lee (2004) A novel magnetic tweezers for manipulation of a single DNA molecule. *17th IEEE Conference on MEMS.* January 25-29. Maastricht, The Netherlands.
20. Li, H. and R. Bashir (2002) Dielectrophoretic separation and manipulation of live and heat-treated cells of Listreria on microfabricated devices with interdigitated electrodes. *Sens. Actuators B Chem.* 86: 215-221.
21. Alivisatos, A. P., K. P. Johnsson, X. Peng, T. E. Wilson, C. J. Loweth, M. P. Bruchez, Jr., and P. G. Schultz (1996) Organization of 'nanocrystal molecules' using DNA. *Nature* 382: 609-611.
22. Mucic, R. C., J. J. Storhoff, C. A. Mirkin, and R. L. Letsinger (1998) DNA-directed synthesis of binary nanoparticle network materials. *J. Am. Chem. Soc.* 120: 12674-12675.
23. Loweth, C. J., W. B. Caldwell, X. Peng, A. P. Alivisatos, and P. G. Schultz (1999) DNA-based assembly of gold nanocrystals. *Angew. Chem. Int. Ed.* 38: 1808-1812.
24. Deng, Z., Y. Tian, S. H. Lee, A. E. Ribbe, and C. Mao (2005) DNA-encoded self-assembly of gold nanoparticles into one-dimensional arrays. *Angew. Chem. Int. Ed.* 44: 3582-3585.
25. Taton, T. A., R. C. Mucic, C. A. Mirkin, and R. L. Letsinger (2000) The DNA-mediated formation of supramolecular mono- and multilayered nanoparticle structures. *J. Am. Chem. Soc.* 122: 6305-6306.
26. Seeman, N. C. (1982) Nucleic acid junctions and lattices. *J. Theor. Biol.* 99: 237-247.
27. Seeman, N. C. (1991) The use of branched DNA for nanoscale fabrication. *Nanotechnology* 2: 149-159.
28. Seeman, N. C., Y. Zhang, and J. Chen (1994) DNA nanoconstructions. *J. Vac. Sci. Technol. A* 12: 1895-1903.
29. Seeman, N. C. (1998) DNA nanotechnology: novel DNA constructions. *Annu. Rev. Biophys. Biomol. Struct.* 27: 225-248.
30. Rothemund, P. W. K., A. Ekani-Nkodo, N. Papadakis, A. Kumar, D. K. Fygenson, and E. Winfree (2004) Design and characterization of programmable DNA nanotubes. *J. Am. Chem. Soc.* 126: 16344-16352.
31. Ekani-Nkodo, A., A. Kumar, and D. K. Fygenson (2004) Joining and scission in the self-assembly of nanotubes from DNA tiles. *Phys. Rev. Lett.* 93: 268301-268304.
32. Sharma, J., R. Chhabra, Y. Liu, Y. Ke, and H. Yan (2006) DNA-templated self-assembly of two-dimensional and periodical gold nanoparticle arrays. *Angew. Chem. Int. Ed.* 45: 730-735.

33. Braun, E., Y. Eichen, U. Sivan, and G. Ben-Yoseph (1998) DNA-templated assembly and electrode attachment of a conducting silver wire. *Nature* 391: 775-778.
34. Keren, K., M. Krueger, R. Gilad, G. Ben-Yoseph, U. Sivan, and E. Braun (2002) Sequence-specific molecular lithography on single DNA molecules. *Science* 297: 72-75.
35. Yan, H., S. H. Park, G. Finkelstein, J. H. Relif, and T. H. LaBean (2003) DNA-templated self-assembly of protein arrays highly conductive nanowires. *Science* 301: 1882-1884.
36. Park, S. H., H. Yan, J. H. Relif, T. H. LaBean, and G. Finkelstein (2004) Electronic nanostructures templated on self-assembled DNA scaffolds. *Nanotechnology* 15: S525-S527.
37. Yan, H., S. H. Park, G. Finkelstein, J. H. Relif, and. T. H. LaBean Materials and Methods, http://www.sciencemag.org/cgi/content/full/301/5641/1882/DC1.
38. Tanaka, K., A. Tengeiji, T. Kato, N. Toyama, and M. Shionoya (2003) A discrete self-assembled metal array in artificial DNA. *Science* 299: 1212-1213.
39. Gu, J., S. Tanaka, Y. Otsuka, H. Tabata, and T. Kawai (2002) Self-assembled dye-DNA network and its photoinduced electrical conductivity. *Appl. Phys. Lett.* 80: 688-690.
40. Won, J., S. K. Chae, J. H. Kim, H. H. Park, Y. S. Kang, and H. S. Kim (2005) Self-assembled DNA composite membranes. *J. Memb. Sci.* 249: 113-117.
41. Hazani, M., F. Hennrich, M. Kappes, R. Naaman, D. Peled, V. Sidorov, and D. Shvarts (2004) DNA-mediated self-assembly of carbon nanotube-based electronic devices. *Chem. Phys. Lett.* 391: 389-392.
42. Li, S., P. He, J. Dong, Z. Guo, and L. Dai (2005) DNA-directed self-assembling of carbon nanotubes. *J. Am. Chem. Soc.* 127: 14-15.
43. Keren, K., R. S. Berman, E. Buchstab, U. Sivan, and E. Braun (2003) DNA-templated carbon nanotube field-effect transistor. *Science* 302: 1380-1382.
44. Sarikaya, M., C. Tamerler, A. K.-Y. Jen, K. Schulten, and F. Baneyx (2003) Molecular biomimetics: nanotechnology through biology. *Nat. Mater.* 2: 577-585.
45. Sarikaya, M., C. Tamerler, D. T. Schwartz, and F. Baneyx (2003) Materials assembly and formation using engineered polypeptides. *Annu. Rev. Mater. Res.* 34: 373-408.
46. Whaley, S. R., D. S. English, E. L. Hu, P. F. Barbara, and A. M. Belcher (2000) Selection of peptides with semiconductor binding specificity for directed nanocrystal assembly. *Nature* 405: 665-668.
47. Brown, S., M. Sarikaya, and E. Johnson (2000) A genetic analysis of crystal growth. *J. Mol. Biol.* 299: 725-735.
48. Naik, R. R., S. J. Stringer, G. Agarwal, S. E. Jones, and M. O. Stone (2002) Biomimetic synthesis and patterning of silver nanoparticles. *Nat. Mater.* 1: 169-172.
49. Kjergaard, K., J. K. Sorensen, M. A. Schembri, and P. Klemm (2000) Sequestration of zinc oxide by fimbrial designer chelators. *Appl. Environ. Microbiol*. 66: 10-14.
50. Nygaard, S., R. Wendelbo, and S. Brown (2002) Surface-specific zeolite-binding proteins. *Adv. Mater.* 14: 1853-1856.
51. Lee, S. W., C. Mao, C. E. Flynn, and A. M. Belcher (2002) Ordering of quantum dots using genetically engineered viruses. *Science* 296: 892-895.
52. Gaskin, D. J. H., K. Starck, and E. N. Vulfson (2000) Identification of inorganic crystal-specific sequences using phage display combinatorial library of short peptides: a feasibility study. *Biotechnol. Lett.* 22: 1211-1216.
53. Scembri, M. A., K. Kjergaard, and P. Klemm (1999) Bioaccumulation of heavy metals by fimbrial designer adhesion. *FEMS Microbiol. Lett.* 170: 363-371.
54. Qin, D., Y. Xia, B. Xu, H. Yang, C. Zhu, and G. M. Whitesides (1999) Fabrication of ordered two-dimensional arrays of micro- and nano-particles using patterned self-assembled monolayers as templates. *Adv. Mater.* 11: 1433-1437.
55. Rao, S. G., L. Huang, W. Setyawan, and S. Hong (2003) Large-scale assembly of carbon nanotubes. *Nature* 425: 36-37.
56. Huang, L., X. Cui, G. Dukovic, and S. P. O'Brien (2004) Self-organizing high-density single-walled carbon nanotube arrays form surfactant suspensions. *Nanotechnology* 15: 1450-1454.
57. Terfort, A., N. Bowden, and G. M. Whitesides (1997) Three-dimensional self-assembly of millimeter-scale components. *Nature* 386: 162-164.
58. Breen, T. L., J. Tien, S. R. J. Oliver, T. Hadzic, and G. M. Whitesides (1999) Design and self-assembly of open, regular, 3D mesostructures. *Science* 284: 948-951.
59. Biebuyck, H. A. and G. M. Whitesides (1994) Self-organization of organic liquids on patterned self-assembled monolayers of alkanethiolates on gold. *Langmuir* 10: 2790-2793.
60. Gracias, D. H., J. Tien, T. L. Breen, C. Hsu, and G. M. Whitesides (2000) Forming electrical networks in three dimensions by self-assembly. *Science* 289: 1170-1172.
61. Jacobs, H. O., A. R. Tao, A. Schwartz, D. H. Gracias, and G. M. Whitesides (2002) Fabrication of a cylindrical display by patterned assembly. *Science* 296: 323-325.
62. Zheng, W. and H. O. Jacobs (2004) Shape-and-solder-directed self-assembly to package semiconductor device segments. *Appl. Phys. Lett.* 85: 3635-3637.
63. Srinivasan, U., D. Liepmann, and R. T. Howe (2001) Microstructure to substrate self-assembly using capillary forces. *J. Microelectromechanical Syst.* 10: 17-24.
64. Trimmer, W. S. (1997) *Micromechanics and MEMS: Classic and Seminal Papers to 1990.* pp. 101-106. Wiley-IEEE Press, New York, NY, USA.
65. Tien, J., A. Terfort, and G. M. Whitesides (1997) Microfabrication through electrostatic self-assembly. *Langmuir* 13: 5349-5355.
66. Lee, S. W., H. A. McNally, D. Guo, M. Pingle, D. E. Bergstrom, and R. Bashir (2002) Electric-field-mediated assembly of silicon islands coated with charged molecules. *Langmuir* 18: 3383-3386.

67. O'Riordan, A., P. Delaney, and G. Redmond (2004) Field configured assembly: programmed manipulation and self-assembly at the mesoscale. *Nano Lett.* 4: 761-765.
68. Heller, M. J. (1996) An active microelectronics device for multiplex DNA analysis. *IEEE Eng. Med. Biol. Mag.* 15: 100-104.
69. Sosnowski, R. G., E. Tu, W. F. Butler, J. P. O'Connell, and M. J. Heller (1997) Rapid determination of single base mismatch mutations in DNA hybrids by direct electric field control. *Proc. Natl. Acad. Sci. USA* 94: 1119-1123.
70. Huang, Y., K. L. Ewalt, M. Tirado, R. Haigis, A. Forster, D. Ackley, M. J. Heller, J. P. O'Connell, and M. Krihak (2001) Electric manipulation of bioparticles and macromolecules on microfabricated electrodes. *Anal. Chem.* 73: 1549-1559.
71. Edman, C, F., R. B. Swint, C. Furtner, R. E. Formosa, S. D. Roh, K. E. Lee, P. D. Swanson, D. E. Ackley, J. J. Coleman, and J. J. Heller (2000) Electric field directed assembly of an InGaA's LED onto silicon circuitry. *IEEE Photo. Technol. Lett.* 12: 1198-1200.
72. Smith, P. A., C. D. Nordquist, T. N. Jackson, T. S. Mayer, B. R. Martin, J. Mbindyo, and T. E. Mallouk (2000) Electric-field assisted assembly and alignment of metallic nanowires. *Appl. Phys. Lett.* 77: 1399-1401.
73. Lee, S. W., H. A. McNally, and R. Bashir (2002) Electric field and charged molecules mediated self-assembly for electronic devices. *Materials Research Society Symposium – Proceedings.* December 2-6. Boston, MA, USA.
74. Lee, S. W. and R. Bashir (2003) Dielectrophoresis and electrohydrodynamics-mediated fluidic assembly of silicon resistors. *Appl. Phys. Lett.* 83: 3833-3835.
75. Derycke, V., R. Martel, J. Appenzeller, and Ph. Avouris (2001) Carbon nanotube inter- and intramolecular logic gates. *Nano Lett.* 1: 453-456.
76. Liu, J., M. J. Casavant, M. Cox, D. A. Walters, P. Boul, W. Lu, A. J. Rimberg, K. A. Smith, D. T. Colbert, and R. E. Smalley (1999) Controlled deposition of individual single-walled carbon nanotubes on chemically functionalized templates. *Chem. Phys. Lett.* 303: 125-129.
77. Umar A., H.-W. Ra, J.-P. Jeong, E.-K. Suh, and Y.-B. Hahn (2006) Synthesis of ZnO nanowires on Si substrate by thermal evaporation method without catalyst: Structural and optical properties. *Kor. J. Chem. Eng.* 23: 499-504.
78. Huang, Y., X. Duan, Q. Wei, and C. M. Lieber (2001) Directed assembly of one-dimensional nanostructures into functional networks. *Science* 291: 630-633.
79. Cui, Y. and C. M. Lieber (2001) Functional nanoscale electronic devices assembled using silicon nanowire building blocks. *Science* 291: 851-853.
80. Joung, H.-A., W.-B. Shim, D.-H. Chung, J. Ahn, B. H. Chung, H.-S. Choi, S.-D. Ha, K.-S. Kim, K.-H. Lee, C.-H. Kim, K.-Y. Kim, and M.-G. Kim (2007) Screening of a specific monoclonal antibody against and detection of *Listeria monocytogenes* whole cells using a surface plasmon resonance biosensor. *Biotechnol. Bioprocess Eng.* 12: 80-85.